Materials Research Bulletin xxx (2016) xxx–xxx

Contents lists available at ScienceDirect

Materials Research Bulletin

journal homepage: www.elsevier.com/locate/matresbu

Crystal structure and microwave dielectric properties of α-$(Ca_{1-x}Sr_x)SiO_3$ ($x = 1$ and 0.8) ring silicates for millimeter-wave applications

Hitoshi Ohsato[a,b,*], Itaru Suzuki[b], Isao Kagomiya[b]

[a] Nagoya Industrial Science Research Institute, Nagoya 464-0819, Japan
[b] Nagoya Institute of Technology, Nagoya 466-8555, Japan

ARTICLE INFO

Article history:
Received 1 August 2016
Received in revised form 16 November 2016
Accepted 16 December 2016
Available online xxx

Keywords:
A. Ceramics
C. X-ray diffraction
D. Crystal structure
D. Dielectric properties

ABSTRACT

Millimeter-wave wireless communications in a high-level information society have been expanding in terms of high-density data transfer and radar for pre-crash safety systems. α-wollastonite ($CaSiO_3$) based and $SrSiO_3$ based solid solutions (s.s.) in the $CaSiO_3$-$SrSiO_3$ eutectic binary system are expected as millimeter-wave dielectrics because of low dielectric constant as described in a previous paper. In this paper, crystal structures of $SrSiO_3$ and $Ca_{0.2}Sr_{0.8}SiO_3$ compounds are analyzed by Rietveld method using X-ray powder diffraction (XRPD) patterns obtained at the PF-KEK, Tsukuba, Japan. Covalencies of Si—O bonds are calculated through the bond strength obtained by the bond length, which at $x = 0.8$ were higher than that of at $x = 1$ as $(Ca_{1-x}Sr_x)SiO_3$. The lowest dielectric constant (ε_r) and highest Qf value at $x = 0.8$ with $\varepsilon_r = 6.62$, $Qf = 66{,}700$ GHz and $\tau_f = -40$ ppm/°C were explained by the covalencies.

1. Introduction

Nikkei Electronics (NE) magazine [1] reported in 2013 that millimeter-wave wireless communication has begun to spread to public welfare systems in Japan. Millimeter-wave communications have reached runways to takeoff after many twists and turns. Wireless gigabite (WiGig) for high data rate communication has the highest data speed of 7 G bits per second at a short communication distance of approximately 10 m, as non compressed millimeter-wave wireless communications [2,3]. Furthermore, millimeter-wave communication can be applied to radar for pre-crash safety systems [4], which are the frequencies assigned by Ministry of Internal Affairs and Communications (MIC) [5].

The dielectrics for millimeter-wave are desired to have high quality factor (Q), low dielectric constant (ε_r) and near-zero temperature coefficients of the resonant frequency (τ_f) [6]. Most of the useful candidate materials with low ε_r and high Qf exist in the silicates [7,8] such as forsterite (Mg_2SiO_4) [9–12], willemite (Zn_2SiO_4) [13], and cordierite/indialite ($Mg_2Al_4Si_5O_{18}$) [14,15]. The low ε_r and high Qf are attributed to the reduced rattling of atoms in the silicate tetrahedra based on covalency [16]. In the case of cordierite/indialite composed of 6-membered SiO_4 hexagonal ring [17], the τ_f shows a value of +24 ppm/°C [18]. High temperature form α-wollastonite $CaSiO_3$ also is a ring silicate [19,20], which is expected to have near zero τ_f. From this point of view, the authors investigated the microwave dielectric properties of α-$CaSiO_3$. The wollastonite possesses two polymorphs [19]: (1) a low-temperature form composed of a chain structure of SiO_4 tetrahedra and (2) a high-temperature form (pseudo-wollastonite: α-$CaSiO_3$) with 3-membered ternary rings of SiO_4 tetrahedra [20]. In addition the authors focused on $SrSiO_3$, where Sr substitutes for Ca, which is composed of 3-membeed ternary ring of SiO_4 tetrahedra [21]. Both α-$CaSiO_3$ and $SrSiO_3$ belong to the same monoclinic space group $C2/c$. However, the detailed structures are different: the former [20] is composed of four layered structure, and latter [21] a six-layered structure.

In a previous paper [22], the authors confirmed α-$CaSiO_3$-$SrSiO_3$ binary phase diagram as shown in Fig. 1 [23], using X-ray powder diffraction, which is constructed by three parts: two solid solutions (s.s.) of $CaSiO_3$ s.s. and $SrSiO_3$ s.s. located $x = 0$ to 0.4 and $x = 0.6$ to 1.0, respectively, and two phase region around $x = 0.5$. The authors also presented the relative densities and microwave dielectric properties of $(Ca_{1-x}Sr_x)SiO_3$ as a function of composition x as shown in Fig. 2 [22]. The quality factor (Qf) shows maximum at $x = 0.8$. In the $CaSiO_3$ s.s. region, the dielectric constants (ε_r) increase with increasing x, depending on the density and the polarizability of the substitutional x value [24]. On the other hand, in the $SrSiO_3$ s.s. region, the ε_r values decrease through to a minimum value. As the polarizability of Sr is larger than that of Ca,

---

[*] Corresponding author at: Nagoya Industrial Science Research Institute, Nagoya 464-0819, Japan.

E-mail addresses: ohsato.hitoshi@gmail.com (H. Ohsato), a_aa_a_00@yahoo.co.jp (I. Suzuki), kagomiya@nitech.ac.jp (I. Kagomiya).

http://dx.doi.org/10.1016/j.materresbull.2016.12.020
0025-5408/© 2016 Elsevier Ltd. All rights reserved.

Please cite this article in press as: H. Ohsato, et al., Crystal structure and microwave dielectric properties of α-$(Ca_{1-x}Sr_x)SiO_3$ ($x = 1$ and 0.8) ring silicates for millimeter-wave applications, Mater. Res. Bull. (2016), http://dx.doi.org/10.1016/j.materresbull.2016.12.020

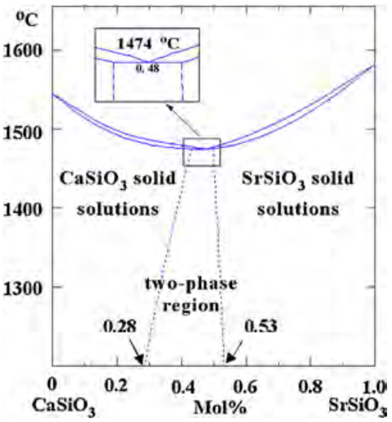

Fig 1. Binary phase diagram of CaSiO$_3$-SrSiO$_3$.

the ε_r of the s.s. should be increased usually as increase of the substitutional x value. Why does the ε_r of the s.s. decrease as x? In this paper, the reason of the abnormal behavior of ε_r, and producing highest Qf value at $x = 0.8$ composition will be clarified based on the crystal structure analyzed by Rietveld method.

2. Experimental

The synthesis of α-CaSiO$_3$, SrSiO$_3$, and (Ca$_{1-x}$Sr$_x$)SiO$_3$ silicate ceramics, and measurement method of densities have been reported in a previous paper [22]. The crystal structure analyses were performed by Rietveld method [25] using the synchrotron radiation powder diffraction data obtained by a multiple 2θ detector system (MDS) [26] at beam line BL-4B2 in the Photon Factory of the High Energy Accelerator Research Organization (PF-KEK), Tsukuba, Japan. The X-ray powder diffraction patterns were obtained in the 2θ range 11–127° using 1.21 Å wave length monochromatized by double-crystal Si(111). The initial data of atomic parameters, space group and lattice parameters were derived from those of SrSiO$_3$ analyzed by Nishi [21].

Bond valence sum (V_i) presented by Brown [27–29] is calculated using following equation:

$$v_{ij} = \exp\left[\frac{R_{ij} - d_{ij}}{b}\right] \qquad (1)$$

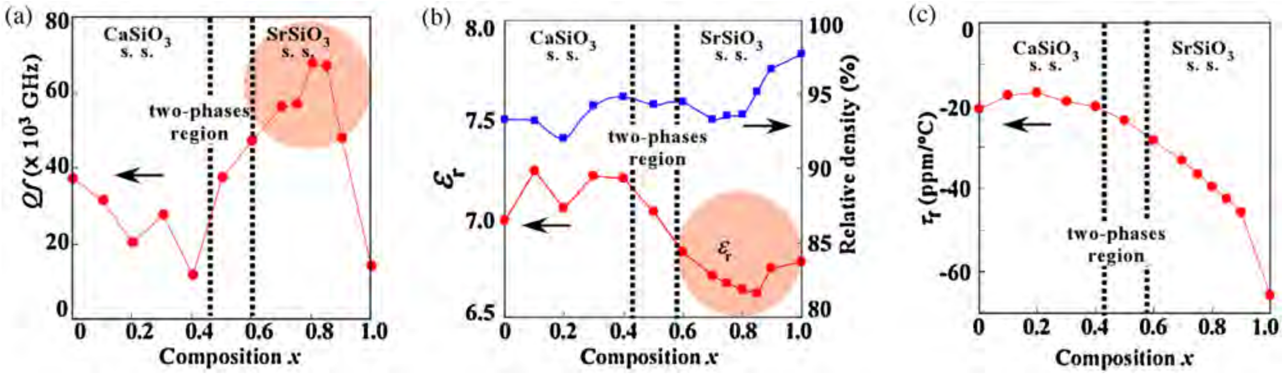

Fig. 2. Relative density and microwave dielectric properties: ε_r, Qf and τ_f as a function of x for (Ca$_{1-x}$Sr$_x$)SiO$_3$.

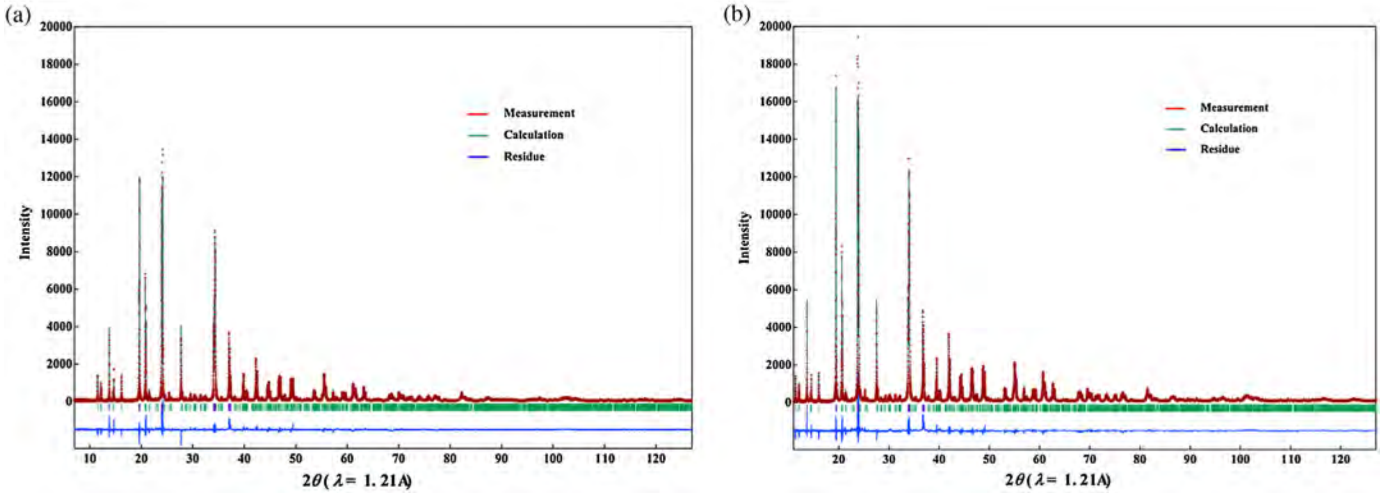

Fig. 3. XRPD patterns of (Ca$_{0.2}$Sr$_{0.8}$)SiO$_3$ (a) and SrSiO$_3$ (b) refined by Rietveld method, which are obtained in the 2θ 11 to 127° using 1.21 Å wave length by synchrotron radiation.

Please cite this article in press as: H. Ohsato, et al., Crystal structure and microwave dielectric properties of α-(Ca$_{1-x}$Sr$_x$) SiO$_3$ (x=1 and 0.8) ring silicates for millimeter-wave applications, Mater. Res. Bull. (2016), http://dx.doi.org/10.1016/j.materresbull.2016.12.020

Table 1
Atomic coordinates and equivalent isotropic temperature factors (origin at −1 on glide plane *c*) of $(Ca_{0.2}Sr_{0.8})SiO_3$ (a) and $SrSiO_3$ (b) with lattice parameters which are same space group of *C*2/*c* (No. 15).

(a)

$Ca_{0.2}Sr_{0.8}SiO_3$

S.G. *C*2/*c* (No.15) monoclinic

$a = 12.250(2)$ Å $b = 7.097(1)$ Å $c = 10.830(1)$ Å $\beta = 111.50(1)^\circ$ $V = 876.0(2)$Å^3

atom	site	*g*	*x*	*y*	*z*	*B*(Å^2)
Sr(1)	8*f*	0.817(2)	0.0865(1)	0.2406(1)	0.4988(1)	0.85(2)
Ca(1)	8*f*	0.183(2)	0.0865(1)	0.2406(1)	0.4988(1)	0.85(2)
Sr(2)	4*c*	0.822(2)	1/4	1/4	0	0.87(3)
Ca(2)	4*c*	0.178(2)	1/4	1/4	0	0.87(3)
Si(1)	8*f*	1	0.1244(2)	0.4545(3)	0.2421(2)	1.34(4)
Si(2)	4*e*	1	0	0.8381(4)	1/4	1.23(7)
O(1)	8*f*	1	0.1363(3)	0.4103(5)	0.1141(4)	0.72(9)
O(2)	8*f*	1	0.2240(3)	0.4020(6)	0.3801(4)	1.40(10)
O(3)	8*f*	1	0.1075(3)	0.6920(5)	0.2495(3)	1.40(12)
O(4)	8*f*	1	0.0529(3)	0.9425(6)	0.3894(3)	0.61(10)
O(5)	4*e*	1	0	0.3574(8)	1/4	1.47(13)

$R_{wp} = 11.17\%$ $R_I = 5.09\%$ $R_F = 2.73\%$ $S = 1.4975\%$

(b)

$SrSiO_3$

S.G. *C*2/*c* (No.15) monoclinic

$a = 12.328(2)$Å $b = 7.143(1)$Å $c = 10.882(2)$Å $\beta = 111.58(1)^\circ$ $V = 891.1(2)$Å^3

atom	site	*x*	*y*	*z*	*B*(Å^2)
Sr(1)	8*f*	0.0865(1)	0.2409(1)	0.4991(1)	0.79(2)
Sr(2)	4*c*	1/4	1/4	0	0.97(4)
Si(1)	8*f*	0.1226(2)	0.4555(4)	0.2416(2)	1.36(5)
Si(2)	4*e*	0	0.8394(5)	1/4	1.68(9)
O(1)	8*f*	0.1358(4)	0.4065(6)	0.1156(4)	0.53(10)
O(2)	8*f*	0.2219(4)	0.3967(7)	0.3791(4)	1.41(12)
O(3)	8*f*	0.1092(3)	0.6929(6)	0.2487(4)	1.43(14)
O(4)	8*f*	0.0530(4)	0.9384(7)	0.3901(4)	0.97(12)
O(5)	4*e*	0	0.3585(9)	1/4	1.45(14)

$R_{wp} = 11.03\%$ $R_I = 2.72\%$ $R_F = 2.08\%$ $S = 1.7939\%$

$$v_i = \Sigma_j \, v_{ij} \tag{2}$$

Here, *i*: No. of cation, *j*: No. of anion, v_{ij}: bond valence between *i* and *j*, R_{ij}: bond valence parameter Ca—O = 1.967, Sr—O = 2.118 and Si—O = 1.624 [30], d_{ij}: atomic distance between no. *i* cation and no. *j* anion, *b*: Empirical parameters (0.37).

The covalency f_c of the cation-oxygen bond was estimated from the following equation [31]:

$$f_c = as^M \tag{3}$$

Where, *a* and *M* are empirical constants, which depend on the number of inner-shell electrons of ions reported by Brown et al. [32]. Here, $a = 0.54$ v.u. and $M = 1.64$ for the inner-shell electrons number 10. The bond strength *s* is obtained from the following equation:

$$s = (d_{ij}/R_I)^{-N} \tag{4}$$

Here, d_{ij} is defined as bond length. R_I and *N* are the empirical parameters that depend on the cation site and the each cation-anion pair, respectively.

Microwave dielectric properties were measured by Hakki and Coleman's method [33,34] in the TE_{011} mode using a network analyzer (Agilent 8720ES). τ_f was measured in the temperature range between 20 and 80 °C.

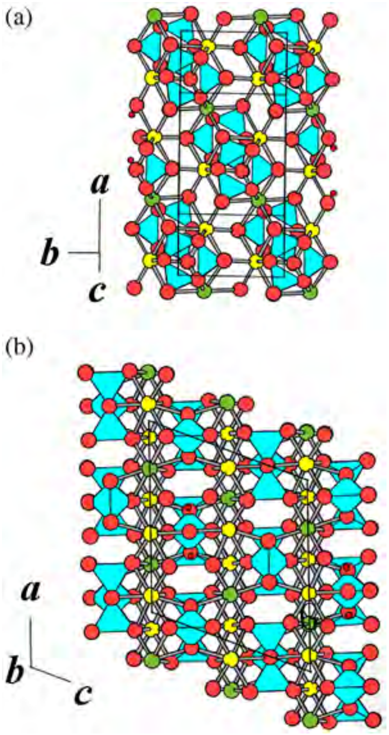

Fig. 4. Crystal structure of $SrSiO_3$. (a) (001) plane with 3-membered rings, (b) projected from *b* unique axis.

Please cite this article in press as: H. Ohsato, et al., Crystal structure and microwave dielectric properties of α-$(Ca_{1-x}Sr_x)SiO_3$ (x=1 and 0.8) ring silicates for millimeter-wave applications, Mater. Res. Bull. (2016), http://dx.doi.org/10.1016/j.materresbull.2016.12.020

Table 2
Volume of MO_8 dodecahedra and SiO_4 tetrahedra, and the differences of Δ in $(Ca_{0.2}Sr_{0.8})SiO_3$ and $SrSiO_3$.

Polyhedra	Volume (Å)		
	$(Ca_{0.2}Sr_{0.8})SiO_3$	$SrSiO_3$	Δ
$M(1)O_8$ dodecahedron	30.75	31.22	−0.47
$M(2)O_8$ dodecahedron	29.82	30.43	−0.61
$Si(1)O_4$ tetrahedron	2.15	2.17	−0.02
$Si(2)O_4$ tetrahedron	2.19	2.24	−0.05

Table 3
Bond lengths, the averages (Å) and the differences Δ of $M—O$ bonds in MO_8 dodecahedra and Si—O bonds in SiO_4 tetrahedra on $(Ca_{0.2}Sr_{0.8})SiO_3$ and $SrSiO_3$.

A		*O*	Bond length of *A*-O (Å)		
			$(Ca_{0.2}Sr_{0.8})SiO_3$	$SrSiO_3$	Δ
M(1)	–	O(1)	2.82	2.82	0
			2.74	2.78	−0.04
	–	O(2)	2.43	2.45	−0.02
			2.72	2.71	0.01
	–	O(3)	2.68	2.67	0.01
	–	O(4)	2.39	2.43	−0.04
			2.75	2.75	0
	–	O(5)	2.64	2.66	−0.02
Average			2.65	2.66	−0.01
M(2)	–	O(1)	2.45	2.47	−0.02
			2.45	2.47	−0.02
	–	O(2)	2.75	2.81	−0.05
			2.75	2.81	−0.05
	–	O(3)	2.67	2.68	−0.01
			2.67	2.68	−0.01
	–	O(4)	2.65	2.65	0
			2.65	2.65	0
Average			2.63	2.65	−0.02
Si(1)	–	O(1)	1.48	1.48	0
	–	O(2)	1.59	1.60	−0.01
	–	O(3)	1.70	1.71	0
	–	O(5)	1.70	1.70	0.01
Average			1.62	1.62	0
Si(2)	–	O(3)	1.68	1.71	−0.03
	–	O(3)	1.68	1.71	−0.03
	–	O(4)	1.59	1.59	0
	–	O(4)	1.59	1.59	0
Average			1.63	1.65	−0.01

Bond			Bond length of *A*-O (Å)		
			$(Ca_{0.2}Sr_{0.8})SiO_3$	$SrSiO_3$	Δ
M(1)	–	O(1)	2.82	2.82	0
			2.74	2.78	−0.04
	–	O(2)	2.43	2.45	−0.02
			2.72	2.71	0.01
	–	O(3)	2.68	2.67	0.01
	–	O(4)	2.39	2.43	−0.04
			2.75	2.75	0
	–	O(5)	2.64	2.66	−0.02
Average			2.65	2.66	−0.01
M(2)	–	O(1)	2.45	2.47	−0.02
			2.45	2.47	−0.02
	–	O(2)	2.75	2.81	−0.05
			2.75	2.81	−0.05
	–	O(3)	2.67	2.68	−0.01
			2.67	2.68	−0.01
	–	O(4)	2.65	2.65	0
			2.65	2.65	0
Average			2.63	2.65	−0.02
Si(1)	–	O(1)	1.48	1.48	0
	–	O(2)	1.59	1.60	−0.01
	–	O(3)	1.70	1.71	0
	–	O(5)	1.70	1.70	0.01
Average			1.62	1.62	0
Si(2)	–	O(3)	1.68	1.71	−0.03
	–	O(3)	1.68	1.71	−0.03
	–	O(4)	1.59	1.59	0
	–	O(4)	1.59	1.59	0
Average			1.63	1.65	−0.01

3. Results and discussion

Fig. 3(a) and (b) shows Rietveld refinement [25] of $(Ca_{0.2}Sr_{0.8})SiO_3$ and $SrSiO_3$, respectively. In the both cases, the observed intensity I_o and calculated intensity I_c, showed by the dotted line and the solid line, respectively, are good fitted, and also the 2θ positions are good fitted, as shown on the difference line between I_o and I_c. Table 1(a) and (b) show atomic coordinates of $(Ca_{1-x}Sr_x)SiO_3$ with $x = 0.8$ and 1.0, respectively, analyzed by Rietveld method [25]. The reliability factors R_F corresponding to *R* factor of single crystal analysis, are 2.75 and 2.08%, respectively with good fitness. In the case of $x = 0.8$, site occupancies of Ca and Sr ions are determined on the 8*f* and 4*c* Wyckoff positions, respectively, on the space group *C*2/*c* (No.15) with unique axis *b*, cell choice 1 [35]. The compositions shift a little by 0.02 for *x* to $SrSiO_3$ from nominal composition. Fig. 4 shows crystal structure of $SrSiO_3$ with 3-membered SiO_4 tetrahedra rings: (a) perpendicular to the ring, (b) the side view of the ring.

Table 2 shows polyhedra volumes of $x = 1.0$ and 0.8 such as MO_8 (M = Ca, Sr) dodecahedra and SiO_4 tetrahedra calculated using the atomic coordinates obtained. The volume of MO_8 dodecahedra is reduced by the substitution for Sr by Ca with small ionic radius. And that of SiO_4 tetrahedra also reduced, in spite of no substitution. Table 3 shows the bond lengths of cation-oxygen on the $x = 0.8$ and 1.0 based on the atomic coordinates obtained. In the case of $x = 0.8$, in spite of small volume on all sites, some bond lengths between center cations and oxygen anions are larger than those of $x = 1.0$. The authors have considered the difference of the bond lengths which is dependent on the bond strength. Therefore, bond valence sum of center atoms on the polyhedra has been calculated as shown in Table 4. The values of MO_8 dodecahedra are almost correspond to the ideal one of 2.0 on the both compositions. But

Table 4
Bond valence sum of $M—O$ bonds in MO_8 dodecahedra and Si —O bonds in SiO_4 tetrahedra on $(Ca_{0.2}Sr_{0.8})SiO_3$ and $SrSiO_3$.

Bond			Bond valance sum	
			$(Ca_{0.2}Sr_{0.8})SiO_3$	$SrSiO_3$
M(1)	–	O(1)	0.141	0.150
			0.175	0.165
	–	O(2)	0.404	0.409
			0.185	0.203
	–	O(3)	0.208	0.226
	–	O(4)	0.455	0.434
			0.168	0.180
	–	O(5)	0.228	0.232
Sum			1.965	2.000
M(2)	–	O(1)	0.379	0.383
			0.379	0.383
	–	O(2)	0.168	0.155
			0.168	0.155
	–	O(3)	0.214	0.221
			0.214	0.221
	–	O(4)	0.225	0.240
			0.225	0.240
Sum			1.974	1.997
Si(1)	–	O(1)	1.476	1.471
	–	O(2)	1.101	1.060
	–	O(3)	0.806	0.797
	–	O(5)	0.808	0.824
Sum			4.191	4.152
Si(2)	–	O(3)	0.866	0.794
	–	O(3)	0.866	0.794
	–	O(4)	1.095	1.106
		O(4)	1.095	1.106
Sum			3.923	3.800

Please cite this article in press as: H. Ohsato, et al., Crystal structure and microwave dielectric properties of α-$(Ca_{1-x}Sr_x)SiO_3$ (x=1 and 0.8) ring silicates for millimeter-wave applications, Mater. Res. Bull. (2016), http://dx.doi.org/10.1016/j.materresbull.2016.12.020

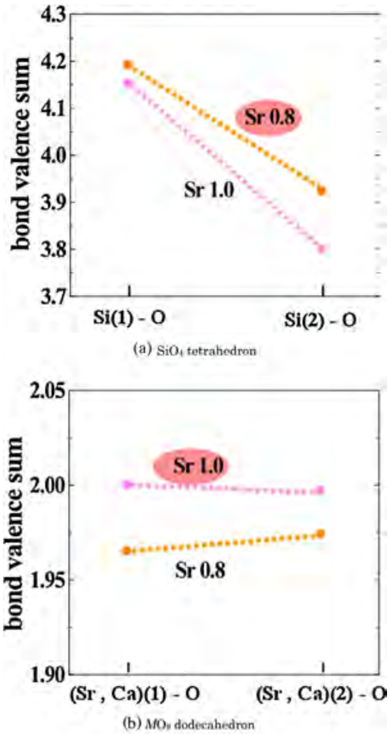

Fig. 5. Bond valence sum of Si-O and *M*-O in SiO_4 tetrahedra (a) and MO_8 dodecahedra (b), respectively, on the $x = 0.8$ and 1.0 for $(Ca_{1\text{-}x}Sr_x)SiO_3$.

Table 5
Covalency (%) of *M*—O bonds in MO_8 dodecahedra and Si—O bonds in SiO_4 tetrahedra on $(Ca_{0.2}Sr_{0.8})SiO_3$ and $SrSiO_3$.

Bond			Covalency (%)	
			$(Ca_{0.2}Sr_{0.8})SiO_3$	$SrSiO_3$
M(1)	–	O(1)	16.09	16.37
			17.95	17.23
	–	O(2)	28.53	28.80
			18.53	19.27
	–	O(3)	19.70	20.45
	–	O(4)	30.59	29.85
			17.60	18.04
	–	O(5)	20.69	20.75
Average			21.21	21.34
M(2)	–	O(1)	27.49	27.67
			27.49	27.67
	–	O(2)	17.62	16.66
			17.62	16.66
	–	O(3)	19.98	20.17
			19.98	20.17
	–	O(4)	20.52	21.11
			20.52	21.11
Average			21.40	21.40
Si(1)	–	O(1)	69.45	69.27
	–	O(2)	57.19	55.81
	–	O(3)	47.18	46.88
	–	O(5)	47.24	47.81
Average			55.26	54.95
Si(2)	–	O(3)	49.27	46.75
	–	O(3)	49.27	46.75
	–	O(4)	56.99	57.36
	–	O(4)	56.99	57.36
Average			53.13	52.06

those of SiO_4 are different from ideal one of 4.0, and the differences are reduced on the $x = 0.8$ as shown visually in Fig. 5. Table 5 shows percentage of the covalency on MO_8 and SiO_4 polyhedra. Those values on MO_8 dodecahedra are almost same value around 21.3%, but on SiO_4 tetrahedra, those values on $x = 0.8$ are larger than those on $x = 1.0$, which are 55.26 and 53.13% on $Si(1)O_4$ and $Si(2)O_4$, respectively. And the difference between $Si(1)O_4$ and $Si(2)O_4$ on $x = 0.8$ is smaller than one on $x = 1.0$.

The microwave dielectric properties of the $(Ca_{1\text{-}x}Sr_x)SiO_3$ solid solutions reported in previous paper [22] are shown in Fig. 2 as described on the Introduction section. The reason showing the highest quality factor (*Qf*) at $x = 0.8$ on the $SrSiO_3$ solid solutions could be explained by the covalency of SiO_4 tetrahedra. As the covalencies of SiO_4 tetraheda at $x = 0.8$ is larger than that at $x = 1.0$ as described in the above paragraph, the crystal structure becomes stable and show the highest *Qf*. An example of improvement of *Qf* based on the covalencies was reported on about new-type corundum [36,37] by Ogawa group in Meijo-University.

The abnormal behavior of ε_r as shown in Fig. 2(b), that is on the $(Ca_{1\text{-}x}Sr_x)SiO_3$, in spite of substitution Sr ions with high polarizability of 4.24 for Ca with that of 3.14 [24], the ε_r values are decreasing, also could be explained by the covalencies obtained. Fig. 6 present the % of covalency of Si(1)-O and Si(2)-O comparing $x = 0.8$ and 1.0. In the case of $x = 0.8$ composition, the % of covalency is larger than that of $x = 1.0$. As the rattling of Si ions in SiO_4 tetrahedra on $x = 0.8$ is reduced by high covalency, the ε_r value is decreased as a function of composition *x* and shows minimum value at $x = 0.8$.

4. Conclusions

There are two points to be clarified on the microwave dielectric properties of α-$CaSiO_3$ based and $SrSiO_3$ based solid solutions obtained on the previous paper [22]. One is the highest *Qf* obtained at $x = 0.8$ in $(Ca_{1\text{-}x}Sr_x)SiO_3$ solid solutions. Another is abnormal dielectric constant behavior on the $(Ca_{1\text{-}x}Sr_x)SiO_3$ solid solutions, that is in spite of substitution Sr with high polarizability for Ca with low one the dielectric constants are decreasing. These points were clarified by the crystal structure analysis of $Ca_{0.2}Sr_{0.8}SiO_3$ ($x = 0.8$) and $SrSiO_3$ ($x = 1.0$). The covalencies of SiO_4 tetrahedra on the $x = 0.8$

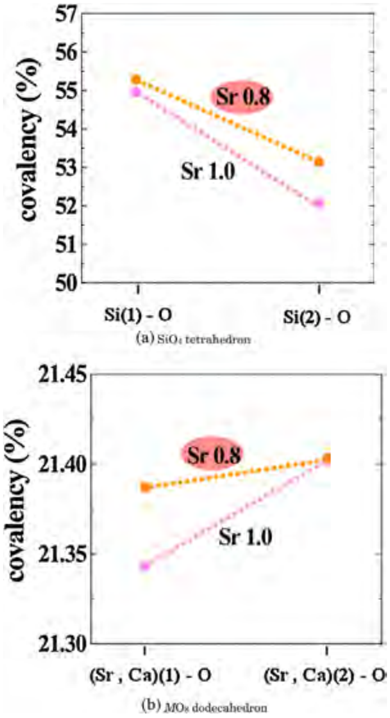

Fig. 6. Covalency (%) of *M*-O and Si-O in SiO_4 tetrahedra (a) and MO_8 dodecahedra (b), respectively, on the $x = 0.8$ and 1.0 for $(Ca_{1\text{-}x}Sr_x)SiO_3$.

Please cite this article in press as: H. Ohsato, et al., Crystal structure and microwave dielectric properties of α-$(Ca_{1\text{-}x}Sr_x)$ SiO_3 ($x = 1$ and 0.8) ring silicates for millimeter-wave applications, Mater. Res. Bull. (2016), http://dx.doi.org/10.1016/j.materresbull.2016.12.020

were higher than those on the $x = 1.0$, which was obtained from crystal structure analyzed by Rietveld method. The high covalencies brings high Qf at $x = 0.8$, decreasing dielectric constants with increasing x in the $SrSiO_3$ solid solutions in spite of increasing of polarizability due to substitution Sr for Ca.

Acknowledgements

The authors would like to thank to Professor Heli Jantunen in University of Oulu in Finland for inviting one of authors as a visiting senior researcher to the University. A part of this work was supported by the Nokia Visiting Professor Foundation, MEXT/JSPS KAKENHI Grant Number 16K06735, and NEDO Foundation “Support program for technology development on the basis of academic findings” by Japanese Ministry of Economy, Trade and Industry.

References

[1] Editor (2013). Take off on WiGig!, Nikkei Electronics, No. 1123 (9 December 2013) 29–49 http://bizboard.nikkeibp.co.jp/kijiken/summary/20131209/NE1123H_2585762a.html [Japanese].
[2] Ed. Nikkei Electronics (2014). Millimeter wave forefront, Nikkei BP, ISBN:978-4-8222-7694-2, [Japanese].
[3] Editor (2008). What is millimeter-wave? J-Net, http://j-net21.smrj.go.jp/develop/digital/entry/001-20081119-06.html/ (Accessed 28 March 2016) [Japanese].
[4] TOYOTA News Release (26 February 2009) http://www.toyota.co.jp/en/news/09/0226.html.
[5] Ministry of Public Management, Home Affairs, Posts and Telecommunications in Japan. http://www.tele.soumu.go.jp/resource/search/myuse/use/ika.pdf, http://www.tele.soumu.go.jp/e/index.htm.
[6] H. Ohsato, Millimeterwave materials, in: M.T. Sebastian, R. Ubic, H. Jantunen (Eds.), Microwave Materials and Applications, John Wiley, New York, 2017.
[7] M.T. Sebastian, Dielectric Materials for Wireless Communication, Elsevier Science Publication, Oxford, 2008.
[8] M.T. Sebastian, R. Ubic, H. Jantunen, Low-loss dielectric ceramic materials and their properties, Int. Mater. Rev. 60 (2015) 395–415.
[9] T. Tsunooka, M. Andou, Y. Higashida, H. Sugiyama, H. Ohsato, Effects of TiO_2 on sinterability and dielectric properties of high-Q forsterite ceramics, J. Euro. Ceram. Soc. 23 (2003) 2573–2578.
[10] T. Tsunooka, H. Sugiyama, K. Kakimoto, H. Ohsato, H. Ogawa, Zero temperature coefficient τ_f and sinterability of forsterite ceramics by rutile addition, J. Ceram. Soc. Jpn. Suppl. 112 (2004) S1637–S1640.
[11] M. Ando, K. Himura, T. Tsunooka, I. Kagomiya, H. Ohsato, Synthesis of high-quality forsterite, Jpn. J. Appl. Phys. 46 (2007) 7112–7116.
[12] M. Ando, H. Ohsato, I. Kagomiya, T. Tsunooka, Quality factor of forsterite for ultrahigh frequency dielectrics depending on synthesis process, Jpn. J. Appl. Phys. 47 (2008) 7729–7731.
[13] Y. Guo, H. Ohsato, K. Kakimoto, Characterization and dielectric behavior of willemite and TiO_2-doped willemite ceramics at millimeter-wave frequency, J. Euro. Ceram. Soc. 26 (2006) 1827–1830.
[14] H. Ohsato, J.-S. Kim, A.-Y. Kim, C.-I. Cheon, K.-W. Chae, Millimeter-wave dielectric properties of cordierite/indialite glass ceramics, Jpn. J. Appl. Phys. 50 (2011) (09NF01-1-5).
[15] H. Ohsato, J.-S. Kim, C.-I. Cheon, I. Kagomiya, Millimeter-wave dielectrics of indialite/cordierite glass ceramics: estimating Si/Al ordering by volume and covalency of Si/Al octahedron, J. Ceram. Soc. Jpn. 121 (2013) 649–654.
[16] H. Ohsato, Microwave materials with high Q and low dielectric constant for wireless communications, Mater. Res. Soc. Symp. Proc. 833 (2005) 55–62.
[17] G.M. Gibbs, Polymorphism of cordierite I, Crystal structure of low cordierite, Am. Mineral. 51 (1966) 1068–1087.
[18] J.-M. Wu, H.-L. Huang, Effect of crystallization on microwave dielectric properties of stoichiometric cordierite glasses containing B_2O_3 and P_2O_5 glasses, J. Mater. Res. 15 (2000) 222–227.
[19] W.A. Deer, R.A. Howie, J. Zussman, Rock-forming Minerals, Single-chain Silicates, 2nd ed., Geological Society Bath, U.K, 1997 (P.547).
[20] H. Yang, C.T. Prewitt, On the crystal structure of pseudowollastonite ($CaSiO_3$), Am. Mineral. 84 (1999) 929.
[21] F. Nishi, Strontium metasilicate, $SrSiO_3$, Acta Cryst. C 53 (1997) 534–536.
[22] I. Kagomiya, I. Suzuki, H. Ohsato, Microwave dielectric properties of $(Ca_{1\text{-}}xSr_x)SiO_3$ ring silicate solid solutions, Jpn. J. Appl. Phys. 48 (2009) (09KE02-1-4).
[23] G.K. Moir, F.P. Glasser, Solid solutions and phase equilibria in the systems Na_2SiO_3-$SrSiO_3$ and Na_2SiO_3-$CaSiO_3$-$SrSiO_3$, Trans. J. Br. Ceram. Soc. 73 (1974) 199–206.
[24] R.D. Shannon, Dielectric polarizabilities of ions in oxides and fluorides, J. Appl. Phys. 73 (1993) 348–366.
[25] F. Izumi, T. Ikeda, A Rietveld-analysis program RIETAN-98 and its applications to zeolites, Mater. Sci. Forum 321–324 (2000) 198–203.
[26] H. Toraya, H. Hibino, K. Ohsumi, A new powder diffractometer for synchrotron radiation with multiple-detector system, J. Synchrotron Radiat. 3 (1996) 75–83.
[27] I.D. Brown, D. Altermatt, Bond-valence parameters obtained from a Systematic analysis of the inorganic crystal structure database, Acta Cryst. B 41 (4) (1985) 244–247.
[28] I.D. Brown, Recent developments in the bond valence model of inorganic bonding, Phy. Chem. Miner. 15 (1987) 30–34.
[29] I.D. Brown, Modeling the structures of lanthanum nickel oxide (La_2NiO_4), Z. krist. 199 (1992) 255–272.
[30] N.E. Brese, M. O’Keefee, Bond-Valence parameters for solids, Acta. Cryst. B 47 (1991) 192–197.
[31] I.D. Brown, R.D. Shannon, Empirical bond-strength-bond-length curves for oxides, Acta Cryst. A 29 (1973) 266–282.
[32] I.D. Brown, K.-K. Wu, Empirical parameters for calculating cation–oxygen bond valences, Acta Cryst. B 32 (1976) 1957–1959.
[33] B.W. Hakki, P.D. Coleman, A dielectric resonator method of measuring inductive in the millimeter range, IRE Trans. Microw. Theory Tech. 8 (1960) 402–410 (MTT).
[34] Y. Kobayasi, M. Kato, Microwave measurement of dielectric properties of low-loss materials by the dielectric resonator method, IEEE Trans. Microw Theory Tech. 33 (1985) 586–592 (MTT).
[35] International table for crystallography, in: Th. Hahn (Ed.), A Space-group Symmetry, fifth edition, The International Union of Crystallography, Springer, 2005.
[36] A. Kan, H. Ogawa, H. Ohsato, Relationship between bond strength and microwave dielectric properties of corundum type $(Mg_{4\text{-}x}Co_x)Nb_2O_9$ and $Mg_4(Nb_{2\text{-}y}Ta_y)O_9$ solid solutions, J. Ceram. Soc. Jpn. Suppl. 112–1 (2004) S1622–S1626.
[37] H. Ogawa, A. Kan, S. Ishihara, Y. Higashida, Crystal structure of corundum type $Mg_4(Nb_{2\text{-}x}Ta_x)O_9$ microwave dielectric ceramics with low dielectric loss, J. Euro. Ceram. Soc. 23 (2003) 2485–2488.

Please cite this article in press as: H. Ohsato, et al., Crystal structure and microwave dielectric properties of α-$(Ca_{1\text{-}x}Sr_x)$ SiO_3 ($x = 1$ and 0.8) ring silicates for millimeter-wave applications, Mater. Res. Bull. (2016), http://dx.doi.org/10.1016/j.materresbull.2016.12.020